Molecular Cell *23*, 925–931, September 15, 2006 ©2006 Elsevier Inc. DOI 10.1016/j.molcel.2006.07.025

Dynamic Regulation of cAMP Synthesis through Anchored PKA-Adenylyl Cyclase V/VI Complexes

Short Article

Andrea L. Bauman,[1] Joseph Soughayer,[1] Bao T. Nguyen,[2] Debbie Willoughby,[3] Graeme K. Carnegie,[1] Wei Wong,[1] Naoto Hoshi,[1] Lorene K. Langeberg,[1] Dermot M.F. Cooper,[3] Carmen W. Dessauer,[2] and John D. Scott[1,*]

[1] Howard Hughes Medical Institute
Vollum Institute, L-474
Oregon Health and Science University
3181 Southwest Sam Jackson Park Road
Portland, Oregon 97239

[2] Department of Integrative Biology and Pharmacology
University of Texas Health Science Center
6431 Fannin, MSB 4.220
Houston, Texas 77030

[3] Department of Pharmacology
Tennis Court Road
University of Cambridge
Cambridge, CB2 1PD
United Kingdom

Summary

Spatiotemporal organization of cAMP signaling begins with the tight control of second messenger synthesis. In response to agonist stimulation of G protein-coupled receptors, membrane-associated adenylyl cyclases (ACs) generate cAMP that diffuses throughout the cell. The availability of cAMP activates various intracellular effectors, including protein kinase A (PKA). Specificity in PKA action is achieved by the localization of the enzyme near its substrates through association with A-kinase anchoring proteins (AKAPs). Here, we provide evidence for interactions between AKAP79/150 and ACV and ACVI. PKA anchoring facilitates the preferential phosphorylation of AC to inhibit cAMP synthesis. Real-time cellular imaging experiments show that PKA anchoring with the cAMP synthesis machinery ensures rapid termination of cAMP signaling upon activation of the kinase. This protein configuration permits the formation of a negative feedback loop that temporally regulates cAMP production.

Introduction

Receptor-G protein-coupled events at the plasma membrane trigger responses that proceed through the generation of cAMP (Lefkowitz, 2004). This soluble second messenger accumulates in cellular microdomains where it locally activates effector proteins such as cAMP-dependent protein kinases (PKA), cAMP phosphodiesterases (PDEs), and cAMP-dependent guanine nucleotide exchange factors (Epacs) (Bos, 2003; Dodge-Kafka et al., 2005; Zaccolo and Pozzan, 2002). AKAPs tether these effector proteins with their downstream targets to facilitate the relay of compartmentalized cAMP signals (Tasken and Aandahl, 2004; Wong and Scott, 2004). AKAPs also influence upstream signaling events by placing cAMP effector proteins in close proximity to β-adrenergic receptors (β-ARs) and the cAMP synthesis machinery (Davare et al., 2001; Fraser et al., 2000; Malbon et al., 2004). We now show that AKAP79/150 anchors PKA close to the ACV and ACVI isoforms to facilitate their preferential phosphorylation. Real-time imaging experiments show that anchoring of PKA to the cAMP synthesis machinery ensures that these signaling events are rapidly terminated upon activation of the kinase.

*Correspondence: scott@ohsu.edu

Results and Discussion

AKAP150 Associates with ACV and ACVI

Because we reasoned that AKAPs might couple PKA to the enzymes that produce cAMP, the agonist forskolin was used as an affinity ligand to purify AC complexes from rat brain (Figure 1A). Proteins were eluted from the affinity resin, and AKAPs were detected by an in vitro overlay procedure using ^{32}P-labeled PKA regulatory subunit (RII) as a probe (Carr et al., 1991). A major RII binding band of 150 kDa was detected in the eluate (Figure 1A, lane 3) that was identified as AKAP150 by immunoblot (Figure 1B, lane 3). The RII (Figure 1C, lane 3) and C subunits (data not shown) of the PKA holoenzyme copurified with AKAP150. The AC isoforms V and/or VI were also detected in the eluate by using an antibody that recognizes both proteins (Figure 1D, lane 3). These protein-protein interactions were confirmed when AC immune complexes (AC1, ACIII, and ACV/VI) isolated from rat brain were probed for copurification of AKAP150 and PKA subunits (Figure 1E). The anchoring protein and RII copurified only with ACV/VI (Figure 1E, lane 5), and C subunit activity was enriched 5.2- ± 0.2-fold (n = 3) in AC V/VI immune complexes over controls (Figure 1F, columns 1 and 2). The ACV/VI-associated PKA activity was blocked by the kinase inhibitor peptide PKI 5-24 (Figure 1F, column 3).

AKAP79-Anchored PKA Modulates AC Activity

AKAP150 and its human ortholog AKAP79 are multivalent anchoring proteins that target PKA, PKC, and the phosphatase PP2B to the inner face of the plasma membrane (Dell'Acqua et al., 1998; Hoshi et al., 2005). AKAP79/150 also interacts with β-ARs in an agonist-independent manner, thereby bringing its anchored enzymes close to ACs (Fraser et al., 2000; Lynch et al., 2005). Previous studies have shown that PKA phosphorylation of ACV or ACVI at a suboptimal consensus site of sequence Lys-Lys-Tyr-Ser-Lys inhibits cAMP synthesis (Chen et al., 1997; Iwami et al., 1995). Therefore, we examined how the anchored PKA affected AC activity inside cells. HEK293 cells were transfected with plasmids encoding both FLAG-tagged AKAP79 and His-tagged ACV. AC activity copurified with AKAP79 immune complexes from cotransfected cells (Figure 1G, column 3), but not from control cells or those expressing AKAP79 alone (Figure 1G, columns 1 and 2). In reciprocal experiments, where both proteins were coexpressed, the immunoprecipitation of ACV-His resulted

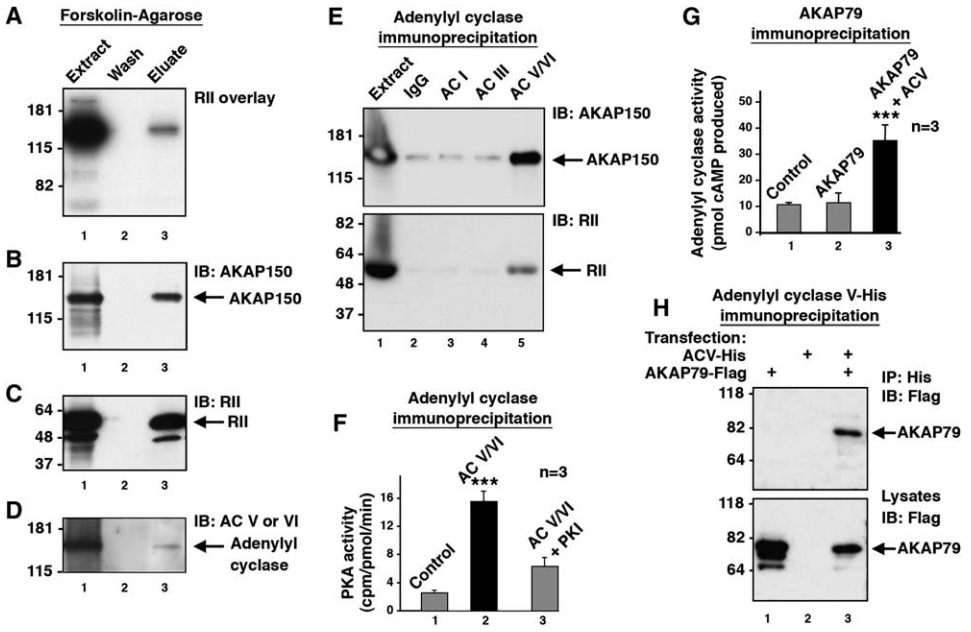

Figure 1. AKAP150 Associates with ACV and ACVI

(A–D) Endogenous AC complexes were isolated from rat brain extract (RBE) by using forskolin-agarose affinity chromatography. Copurifying proteins were identified by RII overlay (A) or Western blots detecting (B) AKAP150, (C) RII, and (D) ACV and ACVI.

(E) Immunoprecipitation of ACs from RBE was performed with antibodies against the ACI, ACII, or ACV/VI isoforms. Immunoblot analysis of each immune complex using anti-AKAP150 (top) and anti-RII (bottom) detected AC-associated proteins.

(F) Measurement of the PKA activity in ACV/VI immune complexes from RBE. Activity measurements were performed with and without the PKA inhibitor PKI. Data are presented as the mean ± SEM from three independent experiments ($p < 0.001$).

(G) Expression of FLAG-tagged AKAP79 alone or in combination with His-tagged ACV in HEK293 cells was followed by anti-FLAG immunoprecipitation of AKAP79. Coprecipitating AC activity was measured upon stimulation with forskolin and $G\alpha_S$-GTPγS. Data are presented as the mean ± SEM, from three independent experiments, each performed in duplicate ($p < 0.001$).

(H) Reciprocal immunoprecipitations using the His tag to isolate ACV complexes were immunoblotted with anti-FLAG to detect coprecipitating AKAP79 (top). The expression levels of FLAG-AKAP79 in cell lysates were determined by immunoblot (bottom).

in the copurification of AKAP79-FLAG (Figure 1H, lane 3). Similar results were obtained with the ACVI isoform (data not shown). Collectively, experiments in Figure 1 suggest that ACV and ACVI form macromolecular complexes with AKAP79/150 and the PKA holoenzyme.

Our working hypothesis was that an anchored pool of PKA suppresses ACV activity. Therefore, intracellular cAMP production was measured by enzyme immunoassay in HEK293 cells expressing $G\alpha_s$QL, a tonically active stimulatory G protein subunit (Figure 2A and Figure S1 in the Supplemental Data available with this article online). Basal levels of cAMP synthesis were measured in control cells and cells expressing recombinant AKAP79 in the presence of the PDE inhibitor IBMX (Figure 2A, columns 1 and 2, and Figure S1). Intracellular cAMP levels were enhanced 2.85- ± 0.3-fold in cells expressing ACV (Figure 2A, column 3), whereas coexpression of AKAP79 or AKAP150 with ACV significantly reduced intracellular cAMP production (Figure 2A, columns 4 and 5). This implies that AKAP79/150 targets PKA toward ACV to repress cAMP synthesis presumably via a mechanism that involves phosphorylation of the cyclase.

In order to test this latter notion, we isolated AC immune complexes from rat brain extracts with the anti-ACV/ACVI antibody. Previous studies have shown that ACV is a predominant isoform in this tissue (Mons and Cooper, 1995). The anchored pool of PKA was activated, and ^{32}P phosphate incorporation was monitored by autoradiography (Figures 2B and 2C). Phosphorylation of ACV was only detected under conditions where PKA was bound to the AKAP prior to activation of the kinase (Figures 2B and 2C, lane 1). Phosphate incorporation was abolished when the immune complexes were incubated with an anchoring inhibitor peptide (AKAP-*IS*) (Alto et al., 2003) prior to activation of the kinase (Figures 2B and 2C, lane 2). Parallel experiments in transfected HEK293 cells confirmed the role of AKAP79-anchored PKA in the phosphorylation of ACV (Figures 2D and 2E). Thus, an anchored pool of PKA phosphorylates ACV. Further support for this notion was provided when ACV activity was measured (as described above) in HEK293 cells expressing AKAP79ΔPKA, a mutant that is unable to anchor PKA. Coexpression of ACV and AKAP79 reduced cAMP production to baseline levels (Figure 2F, columns 1–4), yet maximal ACV activity was retained in cells expressing the AKAP79ΔPKA (Figure 2F, column 5). Additional control experiments showed that ACV activity was unaffected upon expression of AKAP18, an anchoring protein that does not couple to the β2-AR (Figure 2F, column 6).

Previous studies have implicated serine 674 as a regulatory site on ACVI (Chen et al., 1997; Iwami et al., 1995). PKA phosphorylation of this residue suppresses AC activity with a concomitant reduction in cAMP production (Chen et al., 1997; Iwami et al., 1995). Therefore, site-directed mutagenesis techniques were used to introduce a nonphophorylatable side chain at the corresponding site in ACV (position 676). Phosphorylation

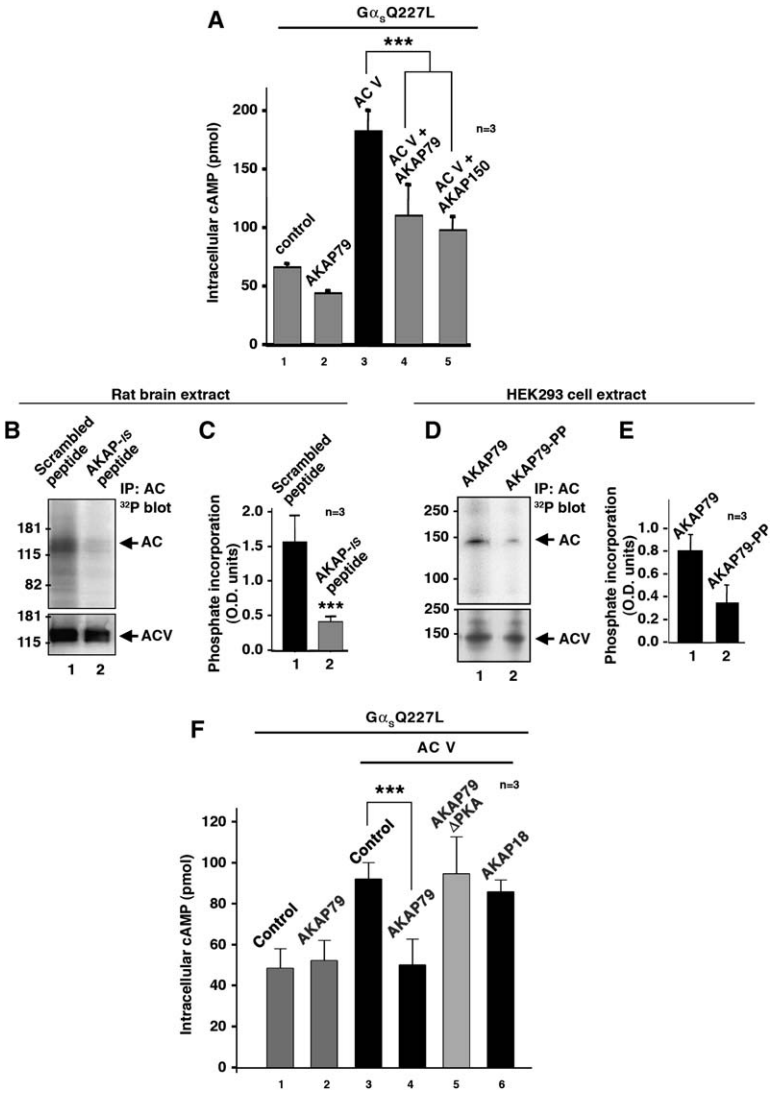

Figure 2. AKAP79-Associated PKA Modulates ACV Activity

(A) HEK293 cells expressing $G\alpha_S$Q227L were transfected with AKAP79 (column 2) or ACV (column 3), AKAP79 and ACV (column 4), or AKAP150 and ACV (column 5). Intracellular cAMP levels were measured by enzyme immunoassay. The data presented are from a single experiment that is representative of three separate experiments, each performed in duplicate. Data are presented as the mean ± SEM; $p < 0.001$.

(B) Endogenous ACV/VI complexes were immunoprecipitated from rat brain extract, and the coprecipitating PKA was activated. Phosphorylation of the precipitated proteins was performed either in the presence of the PKA-anchoring inhibitor, AKAP-*IS* peptide, or the control scrambled AKAP-*IS* peptide. Phosphorylation was monitored by autoradiography of blots to detect incorporation of ^{32}P into AC (top). ACV/VI expression levels were monitored by immunoblot (bottom).

(C) Phosphate incorporation was quantified, and the results were averaged from three independent experiments. Data are presented as the mean ± SEM; $p < 0.001$.

(D) ACV complexes were immunoprecipitated from HEK293 cells coexpressing AKAP79 or the PKA-anchoring defective mutant AKAP79-PP. Coprecipitating PKA was activated with cAMP, and phosphorylation was monitored by autoradiography of blots to detect incorporation of ^{32}P into ACV (top). ACV expression levels were monitored by immunoblot (bottom).

(E) Phosphate incorporation was quantified, and the results were averaged from three independent experiments. Data are presented as the mean ± SEM; $p < 0.001$.

(F) HEK293 cells expressing $G\alpha_S$Q227L, ACV (column 3), ACV and AKAP79 (column 4), ACV and an AKAP79 unable to bind PKA (column 5), or AKAP18 (column 5) were lysed, and cAMP levels in the total cell lysate were measured. Data presented are the average of three separate experiments, each performed in duplicate. Data are presented as the mean ± SEM, $p < 0.001$.

studies confirmed that substitution of Ser-676 with alanine reduced PKA-catalyzed phosphate incorporation into the mutant ACV when compared to a wild-type control (Figure 3A, both panels, and Figure 3b). In addition, AKAP79-mediated suppression of cAMP production was abolished in the ACV S676A mutant when compared to the wild-type protein (Figure 3C). Taken together, these findings support the notion that Ser 676 is a regulatory phosphorylation site on ACV and that it can be modulated by an AKAP79-associated pool of PKA. Collectively, the data in Figures 2 and 3 imply that AKAP79/150 assembles a negative feedback loop that suppresses local cAMP synthesis.

AKAP79 Synchronizes the Modulation of AC Activity in Living Cells

AKAP79 expression was silenced by RNA interference (RNAi) (Figure 4A), allowing us to look at altered cAMP dynamics in living cells. These experiments were performed with two different fluorescent reporters. Changes in Fura-2 absorbance indicated cAMP accumulation at the plasma membrane, whereas the genetically encoded AKAR2 reporter monitored dynamic changes in cytoplasmic PKA activity. Calcium influx through cyclic nucleotide-gated (CNG) ion channels is stimulated in response to an increase in cAMP (Flynn et al., 2001). Thus, when coupled with the calcium-sensitive indicator Fura-2 and the PDE inhibitor IBMX, cAMP-selective CNG channel mutants function as real-time biosensors for cAMP accumulation at the plasma membrane (Rich et al., [2000] and Figure 4B). One clear advantage of this approach is that the mutant CNG channel is faster in its response than any other imaging method in use for measuring cAMP, and it is targeted to the plasma membrane where it is in proximity to ACs (Flynn et al., 2001). Furthermore, calcium influx through this mutant CNG channel is not sufficient to alter the activation kinetics of the ACs, which can be inhibited in response to higher levels of extracellular calcium (Mons and Cooper, 1995). Therefore, HEK293 cells were infected with

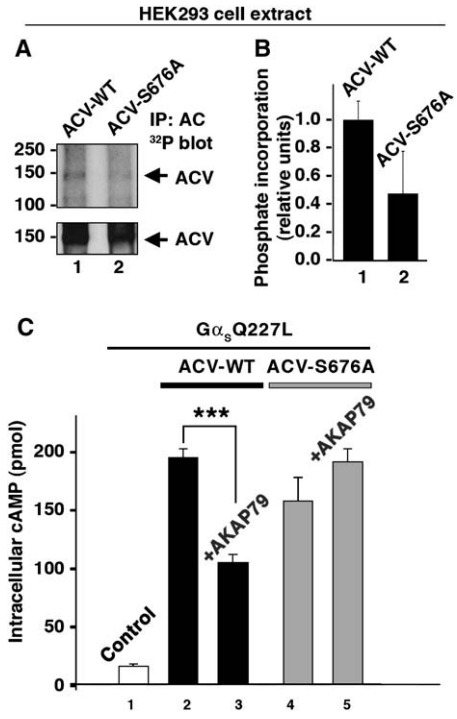

Figure 3. Characterization of the ACV Ser-674 Ala Mutant

(A) (Top) Autoradiograph showing the ^{32}P phosphate incorporation into wild-type ACV (lane 1) and the ACV S676A mutant (lane 2). (Bottom) ACV expression levels were monitored by immunoblot.

(B) Results were quantified by densitometry, and data are presented as the mean ± SEM.

(C) Graph of the levels of intracellular cAMP (pmol) in HEK293 cell lysates expressing the $G\alpha_sQ227L$ constitutively active mutant. Data from cells expressing wild-type ACV (black) and the ACV S67A mutant (gray) are indicated. Data are representative of three separate experiments and are presented as mean ± SEM.

adenovirus encoding a Cys460 Trp, Glu583Met CNG channel mutant and loaded with Fura-2. Changes in Fura-2 emission ratio (F340/380) were measured. A moderate shift in the Fura-2 ratio (F340/380) was detected in control cells upon stimulation of cAMP synthesis with the β-agonist, isoproterenol (30 nM) (Figure 4D, top panels). However, the rate of the response was more pronounced in the AKAP79 knockdown cells (Figure 4D, bottom panels). The amalgamated data from numerous cells are presented in Figure 4C and demonstrate that loss of AKAP79 enhances cAMP accumulation. These effects were not observed in cells with RNAi knockdown of AKAP18 (data not shown).

Complementary experiments examined changes in PKA activity in living cells expressing the AKAR2 reporter (Zhang et al., 2005). AKAR2 is a chimeric protein consisting of cyan fluorescent protein (CFP), a consensus PKA substrate sequence, a Forkhead homology (FHA) domain that binds phosphoamino acids, and the yellow fluorescent protein citrine (Figure 4E). PKA phosphorylation of its consensus site engages the FHA domain to enhance fluorescence resonance energy transfer (FRET) between the fluorescent moieties. HeLa cells expressing AKAR2 were initially stimulated with the specific β2-AR agonist terbutaline (100 μM) for 7 min. The subsequent application of forskolin (20 μM) demonstrated the maximal FRET level. In the absence of PDE inhibitors, the terbutaline promoted an acute and transient elevation of FRET in control cells (Figure 4F, top panels, and Figure 4G, black squares, n = 14). In contrast, the terbutaline response was sustained in AKAP79 knockdown cells (Figure 4F, bottom panels, and Figure 4G, red squares, n = 20). These cells exhibited a slower decay in FRET, and the extent of PKA activity was greater over time (Figure 4H, column 2, and Figure 4I, column 2). Ectopic expression of murine AKAP150, which is refractory to the shRNA, rescued the original FRET response (Figure 4G, green triangles, n = 9; Figure 4H, column 3; and Figure 4I, column 3). Taken together, these FRET measurements imply that AC activity and the concomitant activation of PKA is prolonged in cells lacking AKAP79. Importantly, the cAMP-dependent elevation in FRET was also sustained when cells were rescued with the AKAP150ΔPKA form that is unable to anchor the kinase (Figure 4G, blue circles, n = 9; Figure 4H, column 4; and Figure 4I, column 4). On the basis of these data, we can conclude that AKAP79-anchored PKA participates in the inhibition of AC activity.

Assembly of a Negative Feedback Loop to Regulate Local cAMP Levels

Occupancy of the β-AR triggers cAMP synthesis at spatially resolved locations in the plasma membrane. Our data suggest that AKAP79/150 directs these cAMP signals via PKA toward specific substrates within a β2-AR, G protein, and ACV network. Although biochemical methods were unable to detect Gαs in these macromolecular complexes, a wealth of functional data has demonstrated the dynamic association of this heterotrimeric G protein subunit with the β2-AR and ACs (Lefkowitz, 2004). Ultimately, these events lead to the activation of PKA. Potential substrates for the kinase include the β-AR itself, to switch its coupling to different G proteins (Daaka et al., 1997); and ACV to terminate cAMP production (Chen et al., 1997; Iwami et al., 1995). The net effect of both phosphorylation events is to provide negative feedback on ACV and generate bursts of cAMP synthesis. Our FRET-based PKA activity measurements suggest that this is a fairly rapid process that can return to baseline within 4 min of β2-AR stimulation (Figure 4G). Furthermore, our RNAi experiments imply that AKAP79/150 signaling complexes shape the dynamics of cAMP production. Removal of this anchoring protein not only affects the magnitude of cAMP synthesis as assessed by Fura-2 imaging but also prolongs the duration of cellular PKA activity as measured by the FRET reporter. Rescue with AKAP forms that are unable to tether the kinase sustains PKA activity, which is likely a consequence of persistent cAMP synthesis. It is possible that AKAP79/150 or other anchoring proteins may perform analogous functions for other AC isoforms. In addition, other signaling enzymes that interact with AKAP79/150 may function to regulate cAMP synthesis, such as protein kinase C (PKC) isoforms that have been implicated in the activation of ACV and the inhibition of ACVI (Lai et al., 1997; Mons and Cooper, 1995). Anchored pools of PKC may also participate in the modulation of several other AC isoforms (Mons and Cooper, 1995). These regulatory processes are likely to augment other mechanisms that terminate conventional β2-AR signaling, such as desensitization of the receptor through

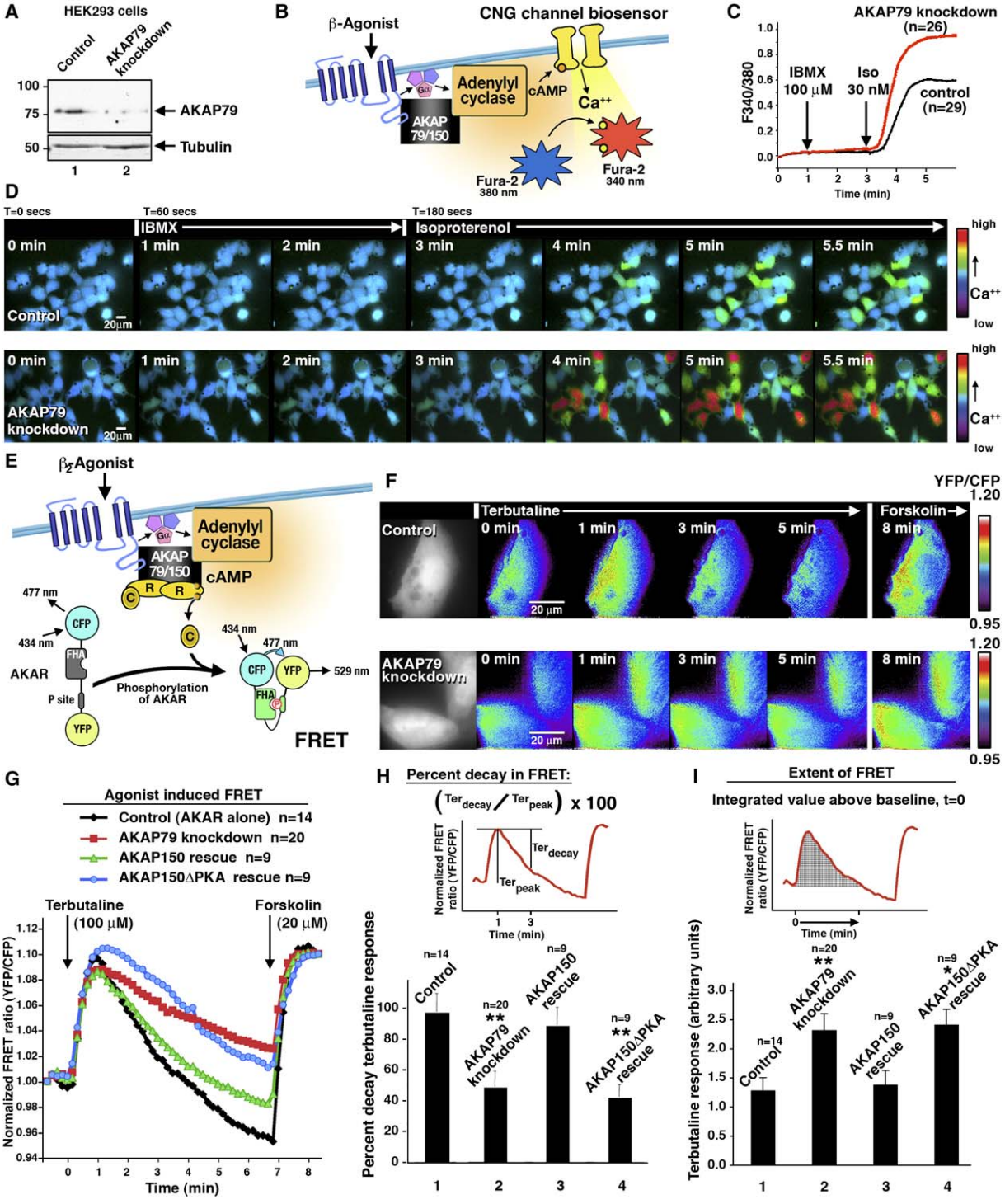

Figure 4. AKAP79 Synchronizes the Modulation of ACV Activity in Living Cells

(A) Silencing of AKAP79 expression in HEK293 cells was confirmed by immunoblot (top). Immunoblot for tubulin is the loading control (bottom).

(B) Schematic diagram of a biosensor for cAMP production by AC in living cells. Activation of β-AR leads to activation of AC and cAMP production. In the presence of a PDE inhibitor, cAMP accumulates near the plasma membrane. A mutant CNG channel biosensor responds to cAMP, permitting calcium entry into Fura-2-loaded cells. The resulting shift in Fura-2 excitation (F340/380) is used to assess cAMP production.

(C) Comparison of cAMP production in AKAP79-silenced cells (red, n = 26) or control cells (black, n = 29) transfected with the biosensor.

(D) Representative pseudocolor images of a field of cells over a time course of 1 min intervals of the data presented in (C).

(E) Schematic diagram of agonist induction of FRET in the PKA activity sensor AKAR2. Signaling from the β-AR leads to activation of AC and an increase in cAMP. Anchored PKA responds to the increased cAMP and phosphorylates AKAR2.

(F) Representative pseudocolored images of FRET changes in control and AKAP79 knockdown HeLa cells (Figure S2) stimulated with terbutaline (t = 0 min) followed with forskolin stimulation (t = 7 min).

recruitment of arrestins (Bohn et al., 1999) and degradation of cAMP by a receptor-associated β-arrestin and type 4 PDE complex (Baillie et al., 2005; Lynch et al., 2005; Perry et al., 2002).

The Role of AKAPs in the Control of cAMP Signaling

The opposing actions of ACs and PDE generate intracellular gradients and compartmentalized pools of cAMP (Dodge-Kafka et al., 2005; Zaccolo and Pozzan, 2002). Interestingly, PKA, the principle target of this second messenger actively, participates in the regulation of both enzyme classes. Although this report has focused on the role of PKA to modulate cAMP generation via ACV activity, it has also been shown (Willoughby et al., 2006) that a growing number of AKAPs cluster PKA with PDEs to terminate cAMP signals as they diffuse into the cell (Asirvatham et al., 2004; Dodge et al., 2001; Tasken et al., 2001). For example, mAKAP-anchored PKA phosphorylates PDE4D3 to favor cAMP degradation at the perinuclear membrane (Dodge et al., 2001; Dodge-Kafka et al., 2005). Likewise, AKAP450 performs a similar function at the centrosomes (Tasken et al., 2001), gravin/AKAP250 clusters PKA with PDE4 isotypes close to the plasma membrane (Willoughby et al., 2006), and AKAP149/121 targets the PDE7A isoform to a variety of subcellular locations (Asirvatham et al., 2004; Baillie et al., 2005). These AKAP-PKA-PDE units respond to upstream signals that emanate from GPCR-AC networks, creating a complex and continually changing signaling environment where cAMP levels are unevenly distributed within the cell. Under this scenario, the activation state of cAMP effectors such as PKA, CNG channels, and Epacs is principally governed by their intracellular location. This notion emphasizes a central role for AKAPs in the spatiotemporal control of cAMP signaling and underscores the pleiotrophic nature of this important second messenger.

Experimental Procedures

Antibodies Used for Immunoblotting and Immunoprecipitation

Antibodies used in this experiment are as follows: rabbit polyclonal antibody to AKAP150 (VO88, 1:10,000), mouse monoclonal PKA type II regulatory subunits α and β (BD Transduction Laboratories 1:1000), mouse monoclonal α-actin antibody (Chemicon 1:500), mouse monoclonal MAP2 antibody (clone HM2, Sigma 1:2300), rabbit polyclonal ACV/VI (C-17), ACIII (C-20), ACI (v-20) (Santa Cruz Biotechnology 1:1000), anti-FLAG M2-peroxidase conjugate (Sigma 1:1000). Western blots are representative of experiments performed at least three times.

Cell Culture and Transfections

Cell culture and transfections were performed as previously described (Dodge-Kafka et al., 2005).

Tissue Extract Preparation and Immunoprecipitations

Detailed methods for the preparation of tissue extracts, the immunoprecipitation of ACV-AKAP complexes, and forskolin agarose pull downs are included in the Supplemental Data.

PKA Activity Assay

The coimmunoprecipitated PKA activity was determined as previously described by (Corbin and Reimann, 1974). For PKA phosphorylation of ACV, immunoprecipitation of the ACV complex was performed as described above. After washing with IP buffer, pellets were washed in cold PBS and treated with lambda phosphatase for 30 min. The samples were washed with HSE, incubated for 20 min at 4°C in 200 μl HSE containing 50 μM either AKAP-*IS* or scrambled AKAP-*IS* peptide and washed with HSE. Addition of 0.75 mM cAMP, 75 μM IBMX, 1 mM DTT, 0.2 mM okadaic acid, and 10 μM FK506 in 20 μl of kinase buffer activated coimmunoprecipitated PKA. After incubation for 30 min at 30°C, the pellets were washed, N-ethylmaleimide (NEM) treated, separated by SDS-PAGE, and transferred to nitrocellulose. Incorporated radioactivity was determined by autoradiography. The amount of immunoprecipitated ACV/VI was determined by using the ACV/VI antibody. The amount of ^{32}P incorporation was normalized to the amount of ACV/VI.

AC Activity Assay from Immunoprecipitates

AC activity was determined as previously described (Dessauer, 2002).

Intracellular cAMP Assay

HEK293 cells transfected (36 hr) with pCDNA3, pCDNA3-$G\alpha_s$Q227L (0.25 μg per well), pCDNA3-ACV (0.3 μg per well), and various AKAP constructs (1 μg per well) were starved in DMEM for 6 hr and then treated with phosphodiesterase inhibitor (1 mM IBMX) for 15 min. Treatments were stopped by removal of media and addition of 250 μl lysis buffer (50 mM Tri-HCl [pH 7.4], 4 mM EDTA, 1 mM IBMX, and protease inhibitors). Total cell lysate was heated at 100°C for 10 min, and cAMP levels were detected by enzyme immunoassay (Assay Designs, Ann Arbor, MI). Protein expression levels were determined by immunoblotting.

cAMP Changes Monitored by Ca^{2+} Influx CNG Channels

Knockdown of AKAP79 in HEK293 cells was performed as previously described (Hoshi et al., 2005). Two days later, cells were infected with adenovirus encoding the α subunit of rat olfactory CNG channel with mutations Cys460Trp and Glu583Met. The following day, the CNG channel-expressing cells were enriched for AKAP79-deficient cells and treated with 100 μM IBMX. After loading with Fura-2, the cells were washed and imaged as previously described (Willoughby et al., 2006). Details can be found in the Supplemental Data.

FRET Imaging and Analysis

Cell culture, transfection, and FRET imaging and analysis were done as previously described (Dodge-Kafka et al., 2005).

Statistical Analysis

Statistical tests for PKA, AC activity, and the accumulation of intracellular cAMP were done by using two-tailed unpaired Student's t tests with Excel (Microsoft) and Instat (Graphpad). Statistical tests for the FRET analysis of PKA phosphorylation were done by using the ANOVA-Dunnett Multiple Comparisons Test.

(G) Amalgamated FRET traces for control (black, n = 14), AKAP79 knockdown (red, n = 20), AKAP150 rescue of AKAP79 knockdown (green, n = 9), and rescue with a mutant AKAP150 that does not bind PKA (blue, n = 9). Analysis of the terbutaline response data presented in (F).
(H) Graph depicting the percentage of FRET signal decay (Ter_{decay} / Ter_{peak} × 100) for each cell group. The terbutaline peak response (Ter_{peak}) is the change in FRET from baseline to peak 1 min after application of agonist. The terbutaline decay (Ter_{decay}) is the change in FRET from the peak response to the FRET value at 3 min. The percent decay represents the dynamics of the response for each cell group. The statistical significance of both AKAP79 knockdown versus control and AKAP150ΔPKA rescue versus control was calculated by using the ANOVA-Dunnett Multiple Comparisons Test and the p value for each was <0.01. Error bars indicate SEM.
(I) The extent of elevated FRET analyzed as the integration of values above baseline from the time of application of terbutaline (t = 0) to the last time point above baseline preceding the addition of forskolin. The statistical significance of AKAP79 knockdown versus control was calculated by using the ANOVA-Dunnett Multiple Comparisons Test and the p value was <0.01. The statistical significance of AKAP150ΔPKA rescue versus control was calculated by using the ANOVA-Dunnett Multiple Comparisons Test and the p value was <0.05. Error bars indicate SEM.

Supplemental Data

Supplemental Data include Supplemental Experimental Procedures and two figures and can be found with this article online at http://www.molecule.org/cgi/content/full/23/6/925/DC1/.

Acknowledgments

This work was supported by grants from The Wellcome Trust (D.M.F.C.), Heart and Stroke Foundation of Canada (W.W.), and the National Institutes of Health (GM48231 to J.D.S., GM60419 to C.W.D., and NS045513 to A.L.B.).

Received: January 27, 2006
Revised: April 21, 2006
Accepted: July 18, 2006
Published: September 14, 2006

References

Alto, N.M., Soderling, S.H., Hoshi, N., Langeberg, L.K., Fayos, R., Jennings, P.A., and Scott, J.D. (2003). Bioinformatic design of A-kinase anchoring protein-in silico: a potent and selective peptide antagonist of type II protein kinase A anchoring. Proc. Natl. Acad. Sci. USA *100*, 4445–4450.

Asirvatham, A.L., Galligan, S.G., Schillace, R.V., Davey, M.P., Vasta, V., Beavo, J.A., and Carr, D.W. (2004). A-kinase anchoring proteins interact with phosphodiesterases in T lymphocyte cell lines. J. Immunol. *173*, 4806–4814.

Baillie, G.S., Scott, J.D., and Houslay, M.D. (2005). Compartmentalisation of phosphodiesterases and protein kinase A: opposites attract. FEBS Lett. *579*, 3264–3270.

Bohn, L.M., Lefkowitz, R.J., Gainetdinov, R.R., Peppel, K., Caron, M.G., and Lin, F.T. (1999). Enhanced morphine analgesia in mice lacking beta-arrestin 2. Science *286*, 2495–2498.

Bos, J.L. (2003). Epac: a new cAMP target and new avenues in cAMP research. Nat. Rev. Mol. Cell Biol. *4*, 733–738.

Carr, D.W., Stofko-Hahn, R.E., Fraser, I.D.C., Bishop, S.M., Acott, T.S., Brennan, R.G., and Scott, J.D. (1991). Interaction of the regulatory subunit (RII) of cAMP-dependent protein kinase with RII-anchoring proteins occurs through an amphipathic helix binding motif. J. Biol. Chem. *266*, 14188–14192.

Chen, Y., Harry, A., Li, J., Smit, M.J., Bai, X., Magnusson, R., Pieroni, J.P., Weng, G., and Iyengar, R. (1997). Adenylyl cyclase 6 is selectively regulated by protein kinase A phosphorylation in a region involved in Galphas stimulation. Proc. Natl. Acad. Sci. USA *94*, 14100–14104.

Corbin, J.D., and Reimann, E.M. (1974). A filter assay for determining protein kinase activity. Methods Enzymol. *38*, 287–294.

Daaka, Y., Luttrell, L.M., and Lefkowitz, R.J. (1997). Switching of the coupling of the beta2-adrenergic receptor to different G proteins by protein kinase A. Nature *390*, 88–91.

Davare, M.A., Avdonin, V., Hall, D.D., Peden, E.M., Burette, A., Weinberg, R.J., Horne, M.C., Hoshi, T., and Hell, J.W. (2001). A beta2 adrenergic receptor signaling complex assembled with the Ca2+ channel Cav1.2. Science *293*, 98–101.

Dell'Acqua, M.L., Faux, M.C., Thorburn, J., Thorburn, A., and Scott, J.D. (1998). Membrane-targeting sequences on AKAP79 bind phosphatidylinositol-4, 5- bisphosphate. EMBO J. *17*, 2246–2260.

Dessauer, C.W. (2002). Kinetic analysis of the action of P-site analogs. Methods Enzymol. *345*, 112–126.

Dodge, K.L., Khouangsathiene, S., Kapiloff, M.S., Mouton, R., Hill, E.V., Houslay, M.D., Langeberg, L.K., and Scott, J.D. (2001). mAKAP assembles a protein kinase A/PDE4 phosphodiesterase cAMP signaling module. EMBO J. *20*, 1921–1930.

Dodge-Kafka, K.L., Soughayer, J., Pare, G.C., Carlisle Michel, J.J., Langeberg, L.K., Kapiloff, M.S., and Scott, J.D. (2005). The protein kinase A anchoring protein mAKAP coordinates two integrated cAMP effector pathways. Nature *437*, 574–578.

Flynn, G.E., Johnson, J.P., Jr., and Zagotta, W.N. (2001). Cyclic nucleotide-gated channels: shedding light on opening of a channel pore. Nat. Rev. Neurosci. *2*, 643–651.

Fraser, I.D., Cong, M., Kim, J., Rollins, E.N., Daaka, Y., Lefkowitz, R.J., and Scott, J.D. (2000). Assembly of an A kinase-anchoring protein-beta(2)-adrenergic receptor complex facilitates receptor phosphorylation and signaling. Curr. Biol. *10*, 409–412.

Hoshi, N., Langeberg, L.K., and Scott, J.D. (2005). Distinct enzyme combinations in AKAP signalling complexes permit functional diversity. Nat. Cell Biol. *7*, 1066–1073.

Iwami, G., Kawabe, J., Ebina, T., Cannon, P.J., Homcy, C.J., and Ishikawa, Y. (1995). Regulation of adenylyl cyclase by protein kinase A. J. Biol. Chem. *270*, 12481–12484.

Lai, H.L., Yang, T.H., Messing, R.O., Ching, Y.H., Lin, S.C., and Chern, Y. (1997). Protein kinase C inhibits adenylyl cyclase type VI activity during desensitization of the A2α-adenosine receptor-mediated cAMP response. J. Biol. Chem. *272*, 4970–4977.

Lefkowitz, R.J. (2004). Historical review: a brief history and personal retrospective of seven-transmembrane receptors. Trends Pharmacol. Sci. *25*, 413–422.

Lynch, M.J., Baillie, G.S., Mohamed, A., Li, X., Maisonneuve, C., Klussmann, E., van Heeke, G., and Houslay, M.D. (2005). RNA silencing identifies PDE4D5 as the functionally relevant cAMP phosphodiesterase interacting with beta arrestin to control the protein kinase A/AKAP79-mediated switching of the beta2-adrenergic receptor to activation of ERK in HEK293B2 cells. J. Biol. Chem. *280*, 33178–33189.

Malbon, C.C., Tao, J., and Wang, H.Y. (2004). AKAPs (A-kinase anchoring proteins) and molecules that compose their G-protein-coupled receptor signalling complexes. Biochem. J. *379*, 1–9.

Mons, N., and Cooper, D.M. (1995). Adenylate cyclases: critical foci in neuronal signaling. Trends Neurosci. *18*, 536–542.

Perry, S.J., Baillie, G.S., Kohout, T.A., McPhee, I., Mageria, M.M., Ang, K.L., Miller, W.E., McLean, A.J., Conti, M., Houslay, M.D., and Lefkowitz, R.J. (2002). Targeting of cyclic AMP degradation to b2-adrenergic receptors by b-arrestins. Science *298*, 834–836.

Rich, T.C., Fagan, K.A., Nakata, H., Schaack, J., Cooper, D.M., and Karpen, J.W. (2000). Cyclic nucleotide-gated channels colocalize with adenylyl cyclase in regions of restricted cAMP diffusion. J. Gen. Physiol. *116*, 147–161.

Tasken, K., and Aandahl, E.M. (2004). Localized effects of cAMP mediated by distinct routes of protein kinase A. Physiol. Rev. *84*, 137–167.

Tasken, K.A., Collas, P., Kemmner, W.A., Witczak, O., Conti, M., and Tasken, K. (2001). Phosphodiesterase 4D and protein kinase a type II constitute a signaling unit in the centrosomal area. J. Biol. Chem. *276*, 21999–22002.

Willoughby, D., Wong, W., Schaack, J., Scott, J.D., and Cooper, D.M. (2006). An anchored PKA and PDE4 complex regulates subplasmalemmal cAMP dynamics. EMBO J. *25*, 2051–2061.

Wong, W., and Scott, J.D. (2004). AKAP signalling complexes: focal points in space and time. Nat. Rev. Mol. Cell Biol. *5*, 959–971.

Zaccolo, M., and Pozzan, T. (2002). Discrete microdomains with high concentration of cAMP in stimulated rat neonatal cardiac myocytes. Science *295*, 1711–1715.

Zhang, J., Hupfeld, C.J., Taylor, S.S., Olefsky, J.M., and Tsien, R.Y. (2005). Insulin disrupts beta-adrenergic signalling to protein kinase A in adipocytes. Nature *437*, 569–573.